# Adsorption performances of the reusable ionic liquid–iron coordination complex (ILICC) adsorbent to remove reactive dyes

Dehong Cheng*, Jie Lin, Sheng Lu, Xu Hao, Yanhua Lu*

*Key Laboratory of Functional Textile Materials, Eastern Liaoning University, Dandong 118000, China, Tel. +86 415 3789976; email: chengdehongldxy@qq.com (D.H. Cheng), Tel. +86 415 3789986; email: linjieln@163.com (J. Lin), Tel. +86 415 3789976; email: lslndd@163.com (S. Lu), Tel. +86 415 3789669; email: cnlnhx@163.com (X. Hao), Tel. +86 415 3789986; Fax: +86 415 3789978; email: yanhualu@aliyun.com (Y.H. Lu)*

**ABSTRACT**

In this paper, the reusable ionic liquid–iron coordination complex (ILICC) adsorbents were synthesized and applied to adsorb reactive dye. Adsorption performances of ILICC as solid-phase adsorbents to remove reactive dye were investigated. The percent of dye removal was 7.0% when 4.0 ml of 0.005 g L$^{-1}$ reactive red B-3BD was directly adsorbed in the neutral condition by 0.02 g of ILICC. The percent of dye removal for the regenerated ILICC was 91.5% when ILICC was reused 10 times. Investigation of adsorption mechanism indicated that the adsorption force was electrostatic interaction between ILICC and reactive red B-3BD dye, and the mode of adsorption was Langmuir adsorption.

*Keywords:* Ionic liquid–iron coordination complex; Reuse; Adsorption; Reactive dye

## 1. Introduction

The development of industry has brought about some serious problems in environmental pollution. Dyeing wastewater is the main pollution source in the printing and dyeing industry. In order to remove dye from dyeing wastewater, some technologies such as liquid–liquid extraction [1], solid-phase adsorption [2], coagulation [3], and biological treatment [4] are adopted to deal with the dyeing wastewater. Among these technologies, the solid-phase adsorption is the conventional method to treat dyeing wastewater. The solid-phase adsorbents including activated carbon [5–9], solid wastes [10,11], TiO$_2$ films [12], and the functional materials [13–19] have been successfully applied to adsorb cationic or anionic dyes.

Ionic liquids as green solvents are broadly applied to remove soluble dyes, reactive dyes, azo dyes, and acid dyes from the dyeing wastewater [20–25]. However, the wastage of ionic liquid is still a problem because ionic liquids dissolve in aqueous solution phase in spite of the recovery technology of ionic liquid being adopted [22].

In order to reduce the wastage, the immobilized ionic liquid on nanoparticles and resin [26,27] are employed to adsorb dyes from the aqueous solution. However, the adsorption capacity of the materials with immobilized ionic liquid was low compared with ionic liquid because the ionic liquids only are immobilized on the surface of materials.

Compared with the immobilized ionic liquid, the ionic liquid–metal coordination complexes include the plentiful ionic liquid groups and show a potential possibility in solid-phase adsorption as adsorbent. It is

*Corresponding authors.

proved that ionic liquid–metal coordination complexes can be prepared through coordination interaction between cation of ionic liquid coordinates and metal ions [28–32], and have been successfully employed to catalyze the synthesis reaction [33,34]. Up to now, ionic liquid–metal coordination complexes have not been applied to the field of solid-phase adsorption.

In this paper, the reusable ionic liquid–iron coordination complexes (ILICC) were prepared and employed as solid-phase adsorbent to adsorb reactive dyes from the aqueous solution. Percent of dye removal, mechanism and mode of removal of the reactive dye were investigated, and the reuse of the regenerated ILICC was determined.

## 2. Experiments

### 2.1. Chemicals

High-quality reactive red B-3BD and reactive blue 19 dyes without any auxiliaries were acquired from Dandong Fuda Chemical Dyes Co., Ltd (Dandong, China). 1-bromooctane and 1-bromobutane (Beijing Chemicals, China), 1-ethylimidazole and 1-methylimidazole (Kaile Chemicals, China) were used as received. ILs 1-butyl-3-methylimizolium bromide, 1-octyl-3-methylimizolium bromide, 1-butyl-3-ethylimizolium bromide, and 1-octyl-3-ethyl imizolium bromide were prepared as reported [21]. 1-methylimidazole and 1-bromobutane with the mole rate 1:1.05 were heated and stirred for 36 h at 80℃, the obtained 1-butyl-3-methylimizolium Bromide (BmimBr) was mixed with active carbon at 70℃ for 1 h with stirring and then was separated by filtration. The colorless ionic liquid BmimBr was used to prepare ILICC. Other chemicals employed were at least of analytical reagent grade and were used without further purification. Deionized water was used throughout.

### 2.2. Synthesis of ILICC

The synthesis process of ILICC was achieved and is shown in Fig. 1. Ionic liquids and ferrous sulfate
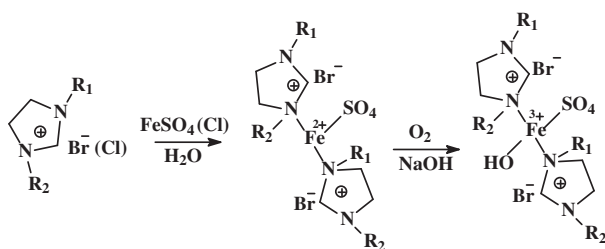
FeSO$_4$ (molar ration for 2:1) were dissolved into the deionized water and stirred at room temperature for 5 h and then heated at 60℃ for 5 h. The yellow flocculent powder was obtained and then washed with the deionized water three times. The obtained yellow powder was mixed with the saturated NaOH solution and then reacted at 60℃ for 5 h. The ILICC with OH and ionic liquids as ligands were prepared and washed with the deionized water five times.

For the purpose of comparison, the ILICC with different alkyl side chains such as 1-butyl-3-ethyl, 1-octyl-3-methyl and 1-octyl-3-ethyl were synthesized according to the aforementioned synthesis process.

### 2.3. Characterization of ILICC

The FT-IR spectra of ILICC were recorded on a Perkin–Elmer FT-IR spectrometer (Wellesley, MA). The resolution is 0.5 cm$^{-1}$. The thermogravimetric analysis of ILICC and reactive dyes were determined using STA 449 F3 Jupiter simultaneous thermal analyzer (DSC/DTA-TG) (Netzsch, Germany). The surface structure of the ILICC powder was observed by a scanning electron microscope (SEM, Hitachi H-600, Japan, 120 kV, 0.26 nm point resolution).

### 2.4. Adsorption process of reactive dyes

0.02 g of ILICC powder was mixed with 4.0 ml of the reactive dye solution with concentration in the range of 0.005–0.025 g L$^{-1}$ in a 5-ml centrifuge tube and then shaken for 10 min using the WH-2 Vortex oscillator (Changzhou Huaao Equipment Manufacture Co., Ltd, China). After centrifugal separation, the concentration of the reactive dye solution was determined by the UV–vis spectrophotometer (Purkinje General Instruments, Beijing, China). After adsorption, the dye concentration was determined based on the absorbance of reactive dyes. The percent of removal ($E$) was calculated based on Eq. (1), where $C_0$ and $C_1$ are the initial and the equilibrium concentrations of the dye in solution (g L$^{-1}$).

$$E = \frac{C_0 - C_1}{C_0} \times 100\% \qquad (1)$$

### 2.5. Regeneration and reuse of ILICC

The ILICCs with the adsorbed reactive dyes were mixed with 4 ml of 0.1 g L$^{-1}$ NaOH solution and then shaken for 10 min. After centrifugal separation ILICC was immersed in the 0.5 g L$^{-1}$ NaOH solution for 1 h.



Fig. 1. Synthesis reaction of ILICC.

The regenerated ILICC was recycled to adsorb reactive dyes according to the aforementioned adsorption process.

## 3. Results and discussion

### 3.1. Characteristics of ILICC

FT-IR spectra of ILICC showed the characteristic bands of imidazolium group were at 3,211, 2,963, and 1,137 cm$^{-1}$, the characteristic band of the $SO_4^{2-}$ group was at 670 nm and the characteristic band of OH group was at about 3,378 cm$^{-1}$.

The TG curve illustrated that mass loss temperature of ILICC with 1-butyl-3-methyl alkyl side chain was about 290℃ and mass change was about −8.22% and the DSC curve showed that the decomposition of ILICC was endothermic and the decomposition temperature was about 296℃.

SEM images of ILICC with different amplification are shown in Fig. 2, which indicates that the size of the ILICC aggregation was about 30 μm and the diameter of the spherical ILICC particle was about 2 μm. The ILICC particle aggregation was scraggy with the villiform ILICC crystals and the large surface area was favored for the adsorption of reactive dye.

### 3.2. Percent of dye removal with ILICC as adsorbent

The effect of the alkyl side chains of ILICC, dye concentration, adsorption time, and adsorption temperature on percent of reactive red B-3BD dye removal was investigated.

### 3.2.1. Effect of alkyl side chain of ILICC on the percent of dye removal

Four ILICCs with 1-butyl-3-methyl, 1-butyl-3-ethyl, 1-octyl-3-methyl, and 1-octyl-3-ethyl side chains were synthesized and the increment of alkyl side chain resulted in the decrement of polarity of ionic liquid groups. 0.02 g of ILICC powder was mixed with 4.0 ml of the reactive dye solution with a concentration of 0.01 g L$^{-1}$ in 5.0-ml centrifuge tube and then shaken for 10 min. The percent of dye removal for these four types of ILICCs as adsorbents was obtained under the same adsorption condition and is shown in Fig. 3. The results indicated when the alkyl side chain was 1-butyl-3-methyl, the percent of dye removal was about 97% and the order of percent of dye removal was 1-butyl-3-methyl > 1-butyl-3-ethyl > 1-octyl-3-methyl > 1-octyl-3-ethyl, which was consistent with that of polarity of ionic liquid groups. The reason may be that the interaction force between ILICC and reactive red B-3BD was reduced when the polarity of ionic liquid groups increased.

### 3.2.2. Effect of reactive dye concentration on percent of dye removal

The percent of dye removal (*E*) of reactive red B-3BD with different concentrations was determined and is shown in Fig. 4. The obtained results indicated that the percent of dye removal was more than 90% when 4.0 ml of reactive red B-3BD with 0.010 g L$^{-1}$ concentration was adsorbed by 0.02 g of ILICC adsorbent. The UV–vis spectra of reactive red B-3BD illustrated that after adsorption the residual reactive dyes almost not existed in dye solution and a quantitative removal of reactive dye could be achieved by applying ILICC as adsorbent.

### 3.2.3. Effect of adsorption time on percent of dye removal

In order to obtain the optimal percent of dye removal the effect of adsorption time was investigated and illustrated in Fig. 5. The result indicated the
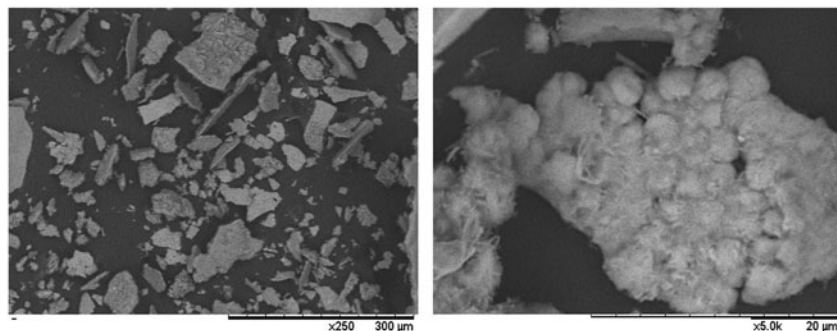


Fig. 2. SEM images of ILICC.
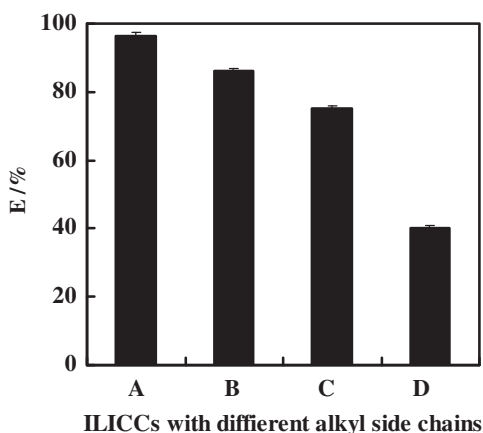
Fig. 3. Percent of dye removal with different ILICCs ((A) 1-butyl-3-methyl alkyl side chain; (B) 1-butyl-3-ethyl alkyl side chain; (C) 1-octyl-3-methyl alkyl side chain; (D) 1-octyl-3-methyl alkyl side chain).



Fig. 5. The percent of dye removal for different adsorption times.

percent of dye removal was 96.5% when 4.0 ml of reactive red B-3BD with 0.010 g L$^{-1}$ concentration was adsorbed by 0.02 g of ILICC for 10 min. The reaction between ILICC and reactive dye was analyzed by applied kinetic equation of the first-order reaction, ln $(C_t/C_0) = kt + C$ ($C_t$ is the concentration of reactive red dye with reaction time $t$. $C_0$ is the initial concentration of dye, $t$ is reaction time and $k$ is the reaction speed constant). The obtained linear relation equation indicated that the adsorption reaction of dye by ILICC belonged to pseudo-first-order reaction. The constant of adsorption rate $k$ was 0.3908 and constant $C$ was 0.7818.

### 3.2.4. Effect of adsorption temperature on the percent of dye removal

The percent of dye removal under different temperatures is shown in Fig. 6. It indicates that the effect of adsorption temperature on the percent of dye removal was obvious, and the percent of dye removal decreased with increasing temperature. Based on the method of the reported literature [35], the linear thermodynamics equation $\ln K = -\Delta H/RT + C$ was calculated and is shown in Fig. 6. The enthalpy change ($\Delta H$) was $-16.60$ kJ based on the equation $-\Delta H/R = 1.9972 \times 10^3$, entropy change ($\Delta S$) was $-37.59$ J K$^{-1}$ based on the equation $\Delta S/R = -4.521$ and free energy change ($\Delta G$) was deduced to be $-5.40$ kJ
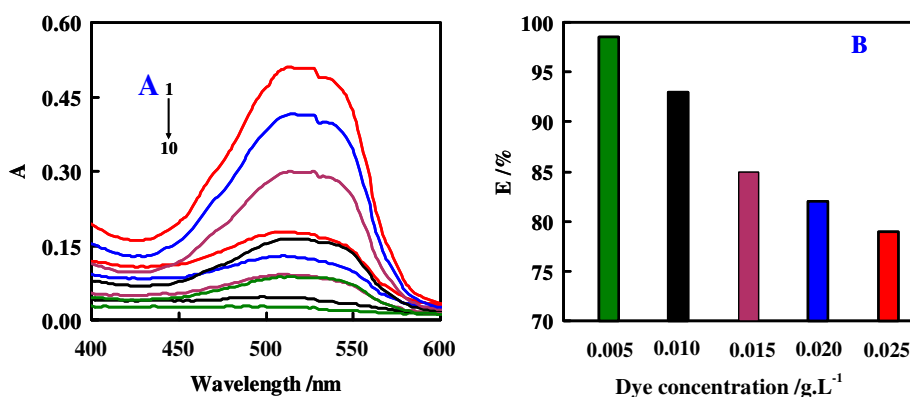


Fig. 4. Absorbance (Fig. 3(A)) and percent of dye removal (Fig. 3(B)) with different concentrations. (1) Before adsorption and (4) after adsorption with 0.025 g l$^{-1}$; (2) before adsorption and (6) after adsorption with 0.020 g l$^{-1}$; (3) before adsorption and (7) after adsorption with 0.015 g l$^{-1}$; (5) before adsorption and (9) after adsorption with 0.010 g l$^{-1}$; (8) before adsorption and (10) after adsorption with 0.005 g l$^{-1}$.
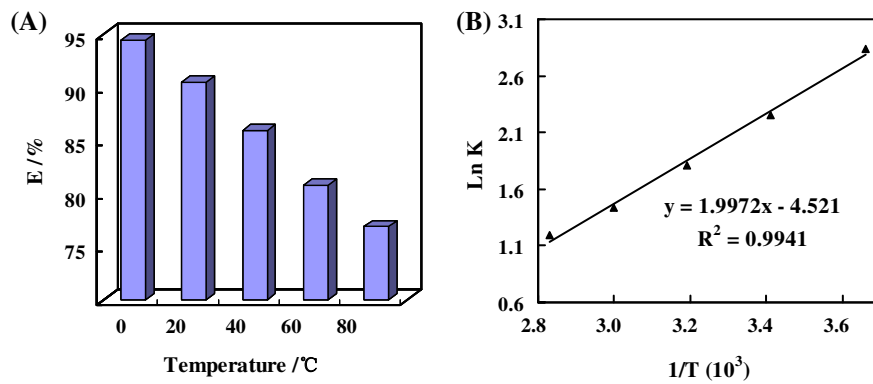
Fig. 6. Percent of dye removal at different temperatures ((1) 0℃; (2) 20℃; (3) 40℃; (4) 60℃; (5) 80℃) (Fig. 5(A)) and the thermodynamics equation (Fig. 5(B)).
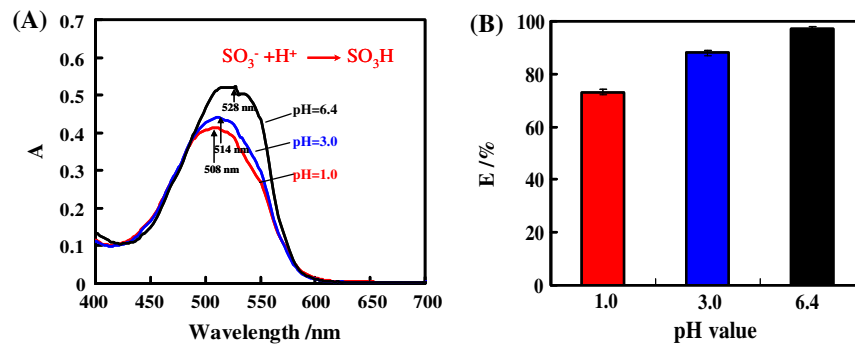


Fig. 7. UV–vis spectra (A) and percent of dye removal (B) at different pH values.

based on the equation $\Delta G = \Delta H - T\Delta S$ (the adsorption temperature was 25℃), indicating that the adsorption of reactive red B-3BD was an exothermic process.

### 3.3. Adsorption mechanism of reactive dye with ILICC as adsorbent

#### 3.3.1. Electrostatic interaction

The $SO_3^-$ group of the reactive red B-3BD dye could interact with $H^+$ to form $SO_3H$ under the acid condition, which was proved by the fact that the maximum adsorption wavelength of the reactive dye varied from 528 to 508 nm when the pH value of reactive dye solution ranged from 6.4 (the deionized water) to 1.0 (Fig. 7). The percent of dye removal at pH 1.0 was less than that at pH 6.4. It could be explained that the $SO_3^-$ group of reactive red B-3BD was favored to interact with $H^+$ ion rather than $Fe^{3+}$ ion of ILICC adsorbent at pH 1.0 (Fig. 8).

When the pH value of the reactive red dye solution was more than 9.0, the percent of dye removal
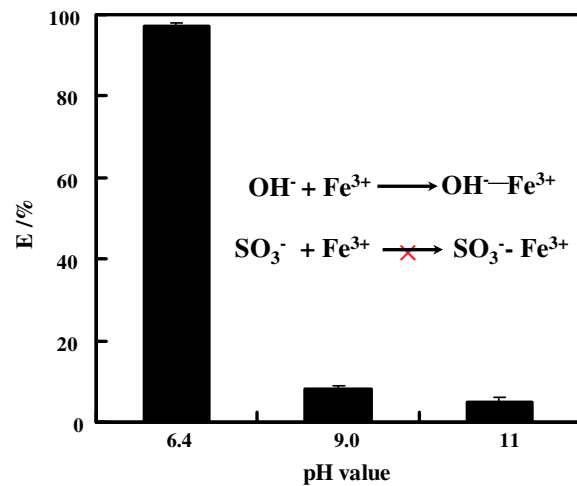


Fig. 8. Percent of dye removal at different pH values.

was 8.0%, less than that at pH 6.4, which indicated that the positive $Fe^{3+}$ ion of ILICC adsorbent was favored to interact with negative $OH^-$ group, rather than the $SO_3^-$ group.
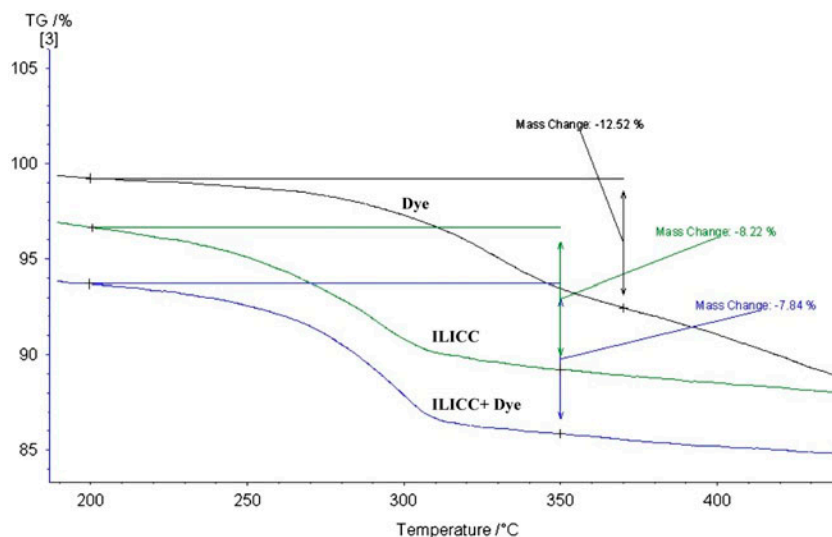
Fig. 9. TG curves of pure ILICC, reactive red B-3BD, and ILICC with the adsorbed reactive red B-3BD.
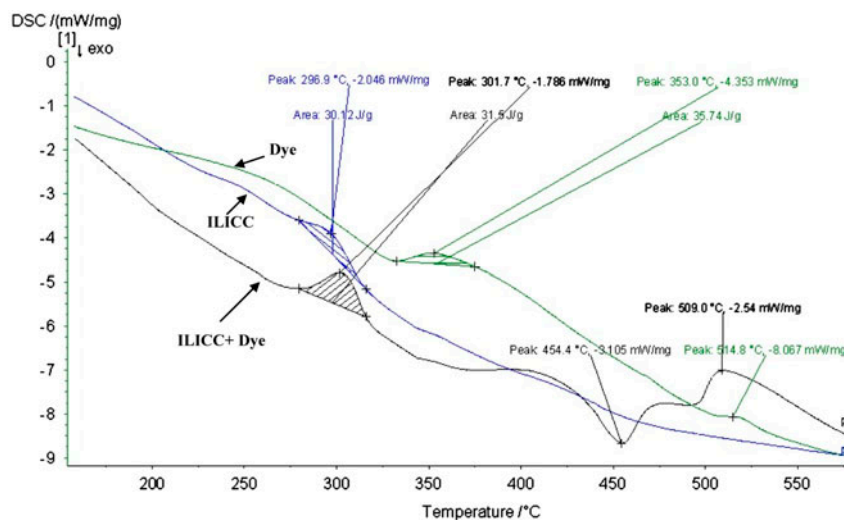


Fig. 10. DSC curves of pure ILICC, reactive red B-3BD and ILICC with the adsorbed reactive red B-3BD.

### 3.3.2. TG curves

TG curves of pure ILICC, reactive red B-3BD and ILICC with the adsorbed reactive red B-3BD are shown in Fig. 9. It illustrates that mass changes of ILICC, reactive red B-3BD, and ILICC with the adsorbed reactive red B-3BD were −8.22, −12.52 and −7.84%, respectively. The mass changes of ILICC with the adsorbed reactive red B-3BD was lowest, which is inadequate with the conventional mass change.

The mass changes of ILICC with the adsorbed reactive red B-3BD should be larger than that of pure ILICC when interactions such as electrostatic and hydrogen bond interactions did not occur. However, the mass changes of ILICC with the adsorbed reactive red B-3BD was the lowest. The reason may be that ILICC interacted with reactive red B-3BD.

### 3.3.3. DSC curves

The DSC curves of ILICC, reactive red B-3BD, and ILICC with the adsorbed reactive red B-3BD are shown in Fig. 10. Decomposition temperature of ILICC
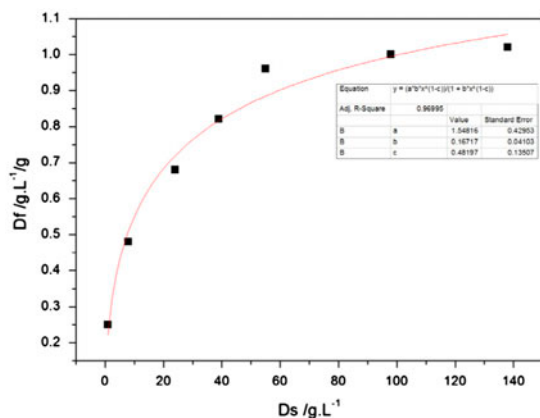
Fig. 11. Adsorption isotherm of reactive red B-3BD with ILICC as adsorbent.

Table 1
Percent of dye removal of the regenerated ILICC

| Reuse time | Mass of the regenerated ILICC (g) | Concentration of reactive dye (g L$^{-1}$) | Percent of dye removal (%) |
| --- | --- | --- | --- |
| 1 | 0.021 | 0.005 | 97.6 |
| 2 | 0.020 | 0.005 | 95.8 |
| 3 | 0.020 | 0.005 | 94.5 |
| 4 | 0.021 | 0.005 | 94.1 |
| 5 | 0.020 | 0.005 | 93.8 |
| 6 | 0.020 | 0.005 | 93.2 |
| 7 | 0.020 | 0.005 | 92.5 |
| 8 | 0.020 | 0.005 | 92.1 |
| 9 | 0.020 | 0.005 | 91.8 |
| 10 | 0.020 | 0.005 | 91.5 |

with the adsorbed reactive red B-3BD was about 301.7°C, higher than 296.9°C of ILICC and less than 353.0°C of reactive red B-3BD, which indicated t hat ILICC interacted with reactive red B-3BD.

### 3.3.4. Mode of adsorption

Based on the dye concentrations of the residual solution $D_s$ and the solid surface $D_f$, the adsorption isotherm of reactive red B-3BD was obtained and is shown in Fig. 11. The Langmuir equation was applied to fit the adsorption isotherm, and the obtained $R^2$ was 0.9699, which illustrated that the mode of adsorption belonged to Langmuir adsorption. Based on the Langmuir equation, the maximum equilibrium adsorption capacity was deduced to be 1.548 and the adsorption constant was deduced to be 0.167.

### 3.4. Regeneration and reuse of ILICC

The NaOH solution was applied to elute the ILICC with the adsorbed reactive dye to regenerate ILICC. The percent of dye removal of the regenerated ILICC is shown in Table 1. The percent of dye removal was 91.5% when the regenerated ILICC was reused 10 times, which indicated ILICC as solid-phase adsorbent not only was reusable but also the percent of dye removal did not reduce.

### 4. Concluding remarks

The use of ILICC as reusable adsorbent to adsorb reactive dyes was investigated. Percent of dye removal of ILICC to remove reactive dyes was determined and through regeneration the ILICC could be recycled to adsorb the reactive dye. A kind of reusable, high-efficiency solid-phase adsorbent was obtained. Compared with the common adsorbents an obvious advantage of the ILICC adsorbent is reusability, and then the other advantage is that ILICC could directly adsorb the reactive dye without any auxiliaries.

### References

[1] P. Pandit, S. Basu, Removal of ionic dyes from water by solvent extraction using reverse micelles, Environ. Sci. Technol. 38 (2004) 2435–2442.
[2] S.A. Dhahir, E. Abdul-Hussein, S.T. Sarhan, N. Faraj, Adsorption of malachite green dye from aqueous solution onto Iraqi Raw Al-Hussainiyat clay, Eur. Chem. Bull. 2 (2013) 866–872.
[3] Y.L. Yuan, Y.Z. Wen, X.Y. Li, S.Z. Luo, Treatment of wastewater from dye manufacturing industry by coagulation, J. Zhejiang Univ. Sci. A 7 (2006) 340–344.
[4] A.O. Dada, A.A. Inyinbor, A.P. Oluyori, Comparative adsorption of dyes onto activated carbon prepared from maize stems and sugar cane stems, IOSR J. Appl. Chem. 3 (2012) 38–43.
[5] M. Shanker, T. Chinniagounder, Adsorption of reactive dye using low cost adsorbent: Cocoa (*Theobroma cacao*) shell, World J. Appl. Environ. Chem. 1 (2012) 22–29.
[6] Y.S. Aldegs, M.I. Elbarghouthi, A.H. Elsheikh, G.M. Walker, Effect of solution pH, ionic strength and temperature on adsorption behavior of reactive dyes on activated carbon, Dyes Pigm. 77 (2008) 16–23.

[7] D.S. Sun, Z.Y. Zhang, M.L. Wang, Y.D. Wu, Adsorption of reactive dyes on activated carbon developed from enteromorpha prolifera, Am. J. Anal. Chem 04 (2013) 17–26.

[8] P.K. Malik, Dye removal from wastewater using activated carbon developed from sawdust: Adsorption equilibrium and kinetics, J. Hazard. Mater. 113 (2004) 81–88.

[9] M. Arulkumar, P. Sathishkumar, T. Palvannan, Optimization of Orange G dye adsorption by activated carbon of *Thespesia populnea* pods using response surface methodology, J. Hazard. Mater. 186 (2011) 827–834.

[10] M.A.M. Salleh, D.K. Mahmoud, W.A.W.A. Karim, A. Idris, Cationic and anionic dye adsorption by agricultural solid wastes: A comprehensive review, Desalination 280 (2011) 1–13.

[11] A.A. Ahmad, A. Idris, B.H. Hameed, Organic dye adsorption on activated carbon derived from solid waste, Desalin. Water Treat. 51 (2013) 2554–2563.

[12] B. O'Regan, L. Xiaoe, T. Ghaddar, Dye adsorption, desorption, and distribution in mesoporous $TiO_2$ films, and its effects on recombination losses in dye sensitized solar cells, Energy Environ. Sci. 5 (2012) 7203–7215.

[13] E.M. Mavioglu Ayan, P. Secim, S. Karakaya, J. Yanik, Oreganum stalks as a new biosorbent to remove textile dyes from aqueous solutions, Clean—Soil, Air, Water 40 (2012) 856–863.

[14] P. Sharma, M.R. Das, Removal of a cationic dye from aqueous solution using graphene oxide nanosheets: Investigation of adsorption parameters, J. Chem. Eng. Data 58 (2013) 151–158.

[15] M. Gharehbaghi, F. Shemirani, A novel method for dye removal: Ionic liquid-based dispersive liquid–liquid extraction (IL-DLLE), Clean—Soil, Air, Water 40 (2012) 290–297.

[16] Y.L. Pang, A.Z. Abdullah, Current status of textile industry wastewater management and research progress in Malaysia: A review, Clean—Soil, Air, Water 41 (2013) 751–764.

[17] C. Umpuch, B. Jutarat, Adsorption of organic dyes from aqueous solution by surfactant modified corn straw, Int. J. Chem. Eng. Appl. 4 (2013) 134–139.

[18] M. Jabli, M.H.V. Baouab, M.S.R.A. Bartegi, Adsorption of acid dyes from aqueous solution on a chitosan-cotton composite material prepared by a new pad-dry process, J. Eng. Fibers Fabr. 6 (2011) 1–12.

[19] S. Patil, S. Renukdas, N. Pate, Removal of methylene blue, removal of methylene blue, a basic dye from aqueous solutions by adsorption using teak tree (Tectona Grandis) bark powder, Int. J. Environ. Sci. 1 (2011) 711–726.

[20] A.M. Ferreira, J.A.P. Coutinho, A.M. Fernandes, M.G. Freire, Complete removal of textile dyes from aqueous media using ionic-liquid-based aqueous two-phase systems, Sep. Purif. Technol. 128 (2014) 58–66.

[21] X.C. Chen, F.L. Li, C. Asumana, G.R. Yu, Extraction of soluble dyes from aqueous solutions with quaternary ammonium-based ionic liquids, Sep. Purif. Technol. 106 (2013) 105–109.

[22] R. Vijayaraghavan, N. Vedaraman, M. Surianarayanan, D.R. MacFarlane, Extraction and recovery of azo dyes into an ionic liquid, Talanta 69 (2006) 1059–1062.

[23] H.L. Chen, S.K. Chang, C.Y. Lee, L.L. Chuang, G.T. Wei, Preconcentration of aqueous dyes through phase-transfer liquid-phase microextraction with a room-temperature ionic liquid, Anal. Chim. Acta 742 (2012) 54–58.

[24] J. Lin, Y. Teng, Y.H. Lu, S. Lu, X. Hao, D.H. Cheng, Usage of hydrophobic ionic liquid [BMIM][$PF_6$] for recovery of acid dye from wastewater and sequential application in Tussah silk dyeing, Clean—Soil, Air, Water 42 (2014) 799–803.

[25] W. Liu, W.J. Zhao, J.B. Chen, M.M. Yang, A cloud point extraction approach using Triton X-100 for the separation and preconcentration of Sudan dyes in chilli powder, Anal. Chim. Acta 605 (2007) 41–45.

[26] T. Poursaberi, M. Hassanisadi, Magnetic removal of Reactive Black 5 from wastewater using ionic liquid grafted-magnetic nanoparticles, Clean—Soil, Air, Water 41 (2013) 1208–1215.

[27] U.A. Qureshi, A.R. Solangi, S.Q. Memon, S.I.H. Taqvi, N. Memon, Ionic liquid modified resin for the adsorptive removal of dibutyl phthalate: Equilibrium, kinetic, and thermodynamic studies, Clean—Soil, Air, Water 40 (2012) 630–639.

[28] E.A. Pidko, V. Degirmenci, R.A. van Santen, E.J. Hensen, Coordination properties of ionic liquid-mediated chromium(II) and copper(II) chlorides and their complexes with glucose, Inorg. Chem. 49 (2010) 10081–10091.

[29] Y. Funasako, M. Nosho, T. Mochida, Ionic liquids from copper(II) complexes with alkylimidazole-containing tripodal ligands, Dalton Trans. 42 (2013) 10138–10143.

[30] H.D. Pratt, A.J. Rose, C.L. Staiger, D. Ingersoll, T.M. Anderson, Synthesis and characterization of ionic liquids containing copper, anganese, or zinc coordination cations, Dalton Trans. 40 (2010) 11396–11401.

[31] W. Lu, P.S. Barber, S.P. Kelley, R.D. Rogers, Coordination and extraction of mercury(II) with an ionic liquid-based thione extractant, Dalton Trans. 42 (2013) 12908–12916.

[32] P. Wasserscheid, C. Hilgers, W. Keim, Ionic liquids-weakly-coordinating solvents for the biphasic ethylene oligomerization to α-olefins using cationic Ni-complexes, J. Mol. Catal. A: Chem. 214 (2004) 83–90.

[33] J. Xiao, B. Twamley, J.M. Shreeve, An Ionic liquid-coordinated palladium complex: A highly efficient and recyclable catalyst for the heck reaction, Org. Lett. 6 (2004) 3845–3847.

[34] D. Zhao, Z. Fei, R. Scopelliti, P.J. Dyson, Synthesis and characterization of ionic liquids incorporating the nitrile functionality, Inorg. Chem. 43 (2004) 2197–2205.

[35] İ. Özbay, U. Özdemir, B. Özbay, S. Veli, Kinetic, thermodynamic, and equilibrium studies for adsorption of azo reactive dye onto a novel waste adsorbent: Charcoal ash, Desalin. Water Treat. 51 (2013) 6091–6100.